0090-9556/10/3805-801–807$20.00
DRUG METABOLISM AND DISPOSITION
Vol. 38, No. 5
32169/3583024
DMD 38:801–807, 2010
Printed in U.S.A.

In Vitro Metabolism and Identification of Human Enzymes Involved in the Metabolism of Methylnaltrexone

Zeen Tong, Appavu Chandrasekaran, Hongshan Li, Yakov Rotshteyn, John C. L. Erve, William DeMaio, Rasmy Talaat, Theresa Hultin, and JoAnn Scatina

Pfizer Inc., Collegeville, Pennsylvania (Z.T., A.C., H.L., J.C.L.E., W.D., R.T., T.H., J.S.); and Progenics Pharmaceuticals, Inc., Tarrytown, New York (Y.R.)

Received January 11, 2010; accepted February 19, 2010

ABSTRACT:

Methylnaltrexone (MNTX) is a peripherally acting μ-opioid receptor antagonist and is currently indicated for the treatment of opioid-induced constipation in patients with advanced illness who are receiving palliative care, when response to laxative therapy has not been sufficient. Sulfation to MNTX-3-sulfate (M2) and carbonyl reduction to methyl-6α-naltrexol (M4) and methyl-6β-naltrexol (M5) are the primary metabolic pathways for MNTX in humans. The objectives of this study were to investigate MNTX in vitro metabolism in human and nonclinical species and to identify the human enzymes involved in MNTX metabolism. Of the five commercially available sulfotransferases investigated, only SULT2A1 and SULT1E1 catalyzed M2 formation. Formation of M4 and M5 was catalyzed by NADPH-dependent hepatic cytosolic enzymes, which were identified using selective chemical inhibitors (10 and 100 μM) for aldo-keto reductase (AKR) isoforms, short-chain dehydrogenase/reductase including carbonyl reductase, alcohol dehydrogenase, and quinone oxidoreductase. The results were then compared with the effects of the same inhibitors on 6β-naltrexol formation from naltrexone, a structural analog of MNTX, which is catalyzed mainly by AKR1C4. The AKR1C inhibitor phenolphthalein inhibited MNTX and naltrexone reduction up to 98%. 5β-Cholanic acid 3α,7α-diol, the AKR1C2 inhibitor, and medroxyprogesterone acetate, an inhibitor of AKR1C1, AKR1C2, and AKR1C4, inhibited MNTX reduction up to 67%. Other inhibitors were less potent. In conclusion, the carbonyl reduction of MNTX to M4 and M5 in hepatic cytosol was consistent with previous in vivo observations. AKR1C4 appeared to play a major role in the carbonyl reduction of MNTX, although multiple enzymes in the AKR1C subfamily may be involved. Human SULT2A1 and SULT1E1 were involved in MNTX sulfation.

Methylnaltrexone (MNTX) is a quaternary derivative of the opioid antagonist naltrexone (Brown and Goldberg, 1985). Unlike naltrexone, this opioid receptor antagonist has restricted penetration across the blood-brain barrier (Brown and Goldberg, 1985; Yuan et al., 1996, 1998). Thus, it reduces the peripheral side effect of opioids without reversal of analgesia or the induction of opioid withdrawal. In healthy volunteers, intravenous MNTX effectively blocked acute morphine-induced delay in oral-cecal transit time without affecting analgesia (Yuan et al., 1996, 2002). A significant reversal of the gut transit delay in subjects dependent on chronic methadone treatment was also observed with intravenous MNTX (Yuan et al., 1998, 1999, 2000). Unlike naltrexone, a structural analog of MNTX without the quaternary amine, which is extensively metabolized in humans (Wall et al., 1981, 1984), MNTX is only minimally metabolized in humans (Chandrasekaran et al., 2010).

It is well documented that sulfation is an important pathway in the biotransformation of xenobiotics such as drugs and endogenous compounds such as thyroid hormones, steroids, monoamine neurotransmitters, and bile acids (Gamage et al., 2006; Matsunaga et al., 2006). Carbonyl reduction of aldehyde and ketone moieties may be catalyzed by alcohol dehydrogenases, aldo-keto reductases (AKRs), short-chain dehydrogenases/reductases (SDRs) including carbonyl reductase (CR), and quinone reductases (Rosemond and Walsh, 2004). Although these enzymes are involved in biological processes such as steroid and prostaglandin metabolism, drug detoxification, housekeeping, stress response, and neurotransmission, and are considered potential drug targets (Rosemond and Walsh, 2004), much less is known about their roles in drug metabolism than their roles in physiological processes. In the present study, in vitro reduction of MNTX was evaluated in mice, rats, dogs, monkeys, and humans, and human enzymes involved in the MNTX metabolism were identified.

Materials and Methods

Materials. [^{14}C]MNTX bromide salt was synthesized by Selcia Limited (Essex, UK). The radiochemical purity and the chemical purity (by UV detection) of the radiolabeled MNTX bromide were greater than 97%. The specific activity was 125.1 μCi/mg (153.0 μCi/mg as the free base). Nonradiolabeled MNTX bromide salt was synthesized by Mallinckrodt Baker, Inc. (Phillipsburg, NJ) and had a chemical purity of 100%. Unless indicated

Progenics Pharmaceuticals, Inc. has a proprietary commercial interest in MNTX. Y.R. is an employee and stockholder of Progenics Pharmaceuticals, Inc.

Article, publication date, and citation information can be found at http://dmd.aspetjournals.org.

doi:10.1124/dmd.110.032169.

ABBREVIATIONS: MNTX, methylnaltrexone; AKR, aldo-keto reductase; SDR, short-chain dehydrogenase/reductase; CR, carbonyl reductase; PAPS, 3′-phosphoadenosine 5′-phosphosulfate lithium salt; HPLC, high-performance liquid chromatography; LC/MS, liquid chromatography/mass spectrometry; M4, methyl-6α-naltrexol; M5, methyl-6β-naltrexol; M2, methylnaltrexone-3-sulfate; P450, cytochrome P450.

otherwise, when referring to [^{14}C]MNTX or MNTX, the free base form is assumed. Naltrexone, 6β-naltrexol hydrate, glucose 6-phosphate, NADP$^+$, and NADPH, 3′-phosphoadenosine 5′-phosphosulfate lithium salt (PAPS), glucose-6-phosphate dehydrogenase, phenolphthalein, flufenamic acid, medroxyprogesterone acetate, indomethacin, phenobarbital, ethacrynic acid, menadione, quercetin, 4-methylpyrazole, and dicumarol were ordered from Sigma-Aldrich (St. Louis, MO). 5β-Cholanic acid-3α,7α-diol was ordered from Steraloids (Newport, RI). Recombinant human SULT1A1, SULT1A2, SULT1A3, SULT2A1, and SULT1E1 were ordered from Invitrogen (Carlsbad, CA). Microsomal and cytosolic fractions of human liver and intestine and hepatic cytosolic fractions of male mouse, rat, dog, and monkey were purchased from XenoTech, LLC (Lenexa, KS). Ultima Gold and Ultima Flo M scintillation mixtures were purchased from PerkinElmer Life and Analytical Sciences (Waltham, MA). ZipTips packed with C18 sorbent were obtained from Millipore Corporation (Billerica, MA). Solvents used for extraction and chromatographic analysis were high-performance liquid chromatography (HPLC) or American Chemical Society reagent grade and were purchased from EMD Chemicals (Gibbstown, NJ). Deuterium oxide and d_4-methanol were obtained from Cambridge Isotope Laboratories, Inc. (Andover, MA).

MNTX Reduction In Vitro. [^{14}C]MNTX was mixed with nonradiolabeled MNTX (1:3 or 1:5) for the incubations. Incubations consisted of [^{14}C]MNTX, magnesium chloride (10 mM), and liver microsomes or cytosol in 0.5 ml of 100 mM potassium phosphate buffer, pH 7.4, and were conducted in a shaking water bath at 37°C. After preincubation for 3 min, the reactions were initiated by the addition of an NADPH-regenerating system. Control incubations were conducted in absence of the NADPH regenerating system. The NADPH-regenerating system consisted of glucose 6-phosphate (2 mg/ml), glucose-6-phosphate dehydrogenase (0.8 units/ml), and NADP$^+$ (2 mg/ml). Incubations were stopped by the addition of 0.5 ml of ice-cold acetonitrile. Samples were vortex-mixed. Denatured proteins were separated by centrifugation at 4300 rpm and 4°C for 10 min (model T21 super centrifuge; Sorvall, Newton, CT). The supernatant was evaporated to a volume of approximately 0.4 ml under a nitrogen stream in a TurboVap LV evaporator (Caliper Life Sciences, Hopkinton, MA). The concentrated sample was centrifuged, and duplicate aliquots (20 μl) of the supernatant were taken for determination of radioactivity by liquid scintillation as described later. This extraction method recovered greater than 85% of the radioactivity from the reaction mixture. An aliquot of the supernatant was analyzed by HPLC with radioactivity flow detection.

MNTX reduction in hepatic microsomal and cytosolic fractions was evaluated in different species. [^{14}C]MNTX (50 μM, 0.3–0.5 μCi/ml) was incubated with liver microsomes or cytosol (4 mg/ml) of mice, rats, dogs, monkeys, and humans for 2 h as described above. Activity in the microsomal and cytosolic fractions in human intestine was also evaluated under the same conditions.

Conditions were optimized for kinetic study in liver cytosol of mice, rats, monkeys, and humans. Time course and protein dependence experiments were conducted to determine the initial rate conditions. The time course study was conducted by incubating [^{14}C]MNTX (50 μM, 0.3 μCi/ml) in the presence of the NADPH-regenerating system with liver cytosol (2.0 mg/ml) for 0, 10, 20, 30, 60, and 120 min under the conditions described above. The protein dependence experiment was conducted by incubating [^{14}C]MNTX (50 μM, 0.3 μCi/ml) for 1 h in the presence of the NADPH-regenerating system with liver cytosol (0, 0.1, 0.25, 0.5, 1.0, 2.0, 4.0, and 6.0 mg/ml) under the conditions described above.

Kinetics of MNTX reduction was determined under the initial rate conditions. In brief, [^{14}C]MNTX (5.0–2000 μM) was incubated in the presence of the NADPH-regenerating system with liver cytosol (0.5–4.0 mg/ml) for 60 to 120 min. The incubation conditions are listed in Table 1. Likewise, time course, protein dependence, and kinetics of naltrexone reduction to 6β-naltrexol in human liver cytosol were also studied under the conditions listed in Table 1 for comparison with MNTX.

Identification of Human Enzymes Involved in MNTX Sulfation. To identify the sulfotransferase isoforms responsible for MNTX sulfation, [^{14}C]MNTX (10 μM, 0.3 μCi/ml) was incubated with the recombinant SULT1A1, SULT1A2, SULT1A3, SULT1E1, and SULT2A1 (0.06–0.23 mg/ml) in the presence of PAPS (25 μM) in 0.5 ml of phosphate buffer, pH 7.4, containing 10 mM $MgCl_2$. PAPS was added to start the reaction after preincubation at 37°C for 3 min. Control incubations lacked PAPS. Incubations were stopped after 1 h by the addition of 0.5 ml of ice-cold acetonitrile.

TABLE 1

Initial rate conditions and incubation conditions used to measure kinetic parameters for MNTX reduction to M4 and M5 in liver cytosol of mice, rats, monkeys, and humans, and for naltrexone reduction to 6β-naltrexol in human liver cytosol

Substrate	Species	Linear Range				Conditions for Kinetic Study		
		Incubation Time		Protein Concentration		Incubation Time	Protein Concentration	MNTX Concentration
		M4	M5	M4	M5			
		min	*min*	*mg/ml*	*mg/ml*	*min*	*mg/ml*	*μM*
MNTX	Mouse	N.A.	0–120	0–6.0	0–6.0	120	4.0	5–2000
	Rat	N.A.	0–120	N.A.	0–6.0	120	4.0	5–5000
	Monkey	0–60	0–60	0–6.0	0–6.0	60	4.0	5–2000
	Human	0–120	0–120	0–4.0	0–4.0	120	1.0	0.5–5000
Naltrexone	Human	0–120		0–0.5		30	0.5	5–1000

N.A., not applicable.

TABLE 2

Selective chemical inhibitors used to identify the enzymes responsible for the carbonyl reduction of MNTX

Chemical Inhibitors	Reductases	References
Phenolphthalein	AKR1C1, 1C2, 1C3, 1C4	(Atalla et al., 2000; Rosemond et al., 2004; Steckelbroeck et al., 2006)
Flufenamic acid	AKR1C1, 1C2, 1C3, 1C4	(Atalla et al., 2000; Rosemond et al., 2004; Steckelbroeck et al., 2004, 2006)
5β-Cholanic acid-3α,7α-diol	AKR1C2	(Steckelbroeck et al., 2006)
Medroxyprogesterone acetate	AKR1C1, 1C2, 1C4	(Atalla et al., 2000)
Indomethacin	AKR1C1, 1C2, 1C3, 1C4, CR	(Gebel and Maser, 1992; Maser et al., 2000; Bauman et al., 2005)
Phenobarbital	AKR1A1(aldehyde reductase) AKR1B1 (aldose reductase)	(Gebel and Maser, 1992; Maser et al., 2000; Rosemond and Walsh, 2004)
Ethacrynic acid	CR/SDR	(Maser et al., 2000; Atalla and Maser, 2001)
Menadione	CR/SDR	(Atalla et al., 2000; Maser et al., 2000; Porter et al., 2000; Atalla and Maser, 2001; Rosemond et al., 2004)
Quercetin	CR/SDR	(Gebel and Maser, 1992; Atalla et al., 2000; Maser et al., 2000; Atalla and Maser, 2001; Rosemond et al., 2004)
4-Methylpyrazole	Alcohol dehydrogenase	(Maser et al., 2000; Atalla and Maser, 2001)
Dicumarol	Quinone oxidoreductase	(Gebel and Maser, 1992; Maser et al., 2000)

Identification of Human Enzymes Involved in MNTX Reduction. To identify the enzymes responsible for the carbonyl reduction of MNTX, [^{14}C]MNTX (500 μM, 0.5 μCi/ml) was incubated with human liver cytosol (4.0 mg/ml) in the presence of the NADPH-regenerating system and a chemical inhibitor (10 and 100 μM; Table 2) for 2 h under the conditions described above. Quercetin was dissolved in 10% dimethyl sulfoxide in methanol;

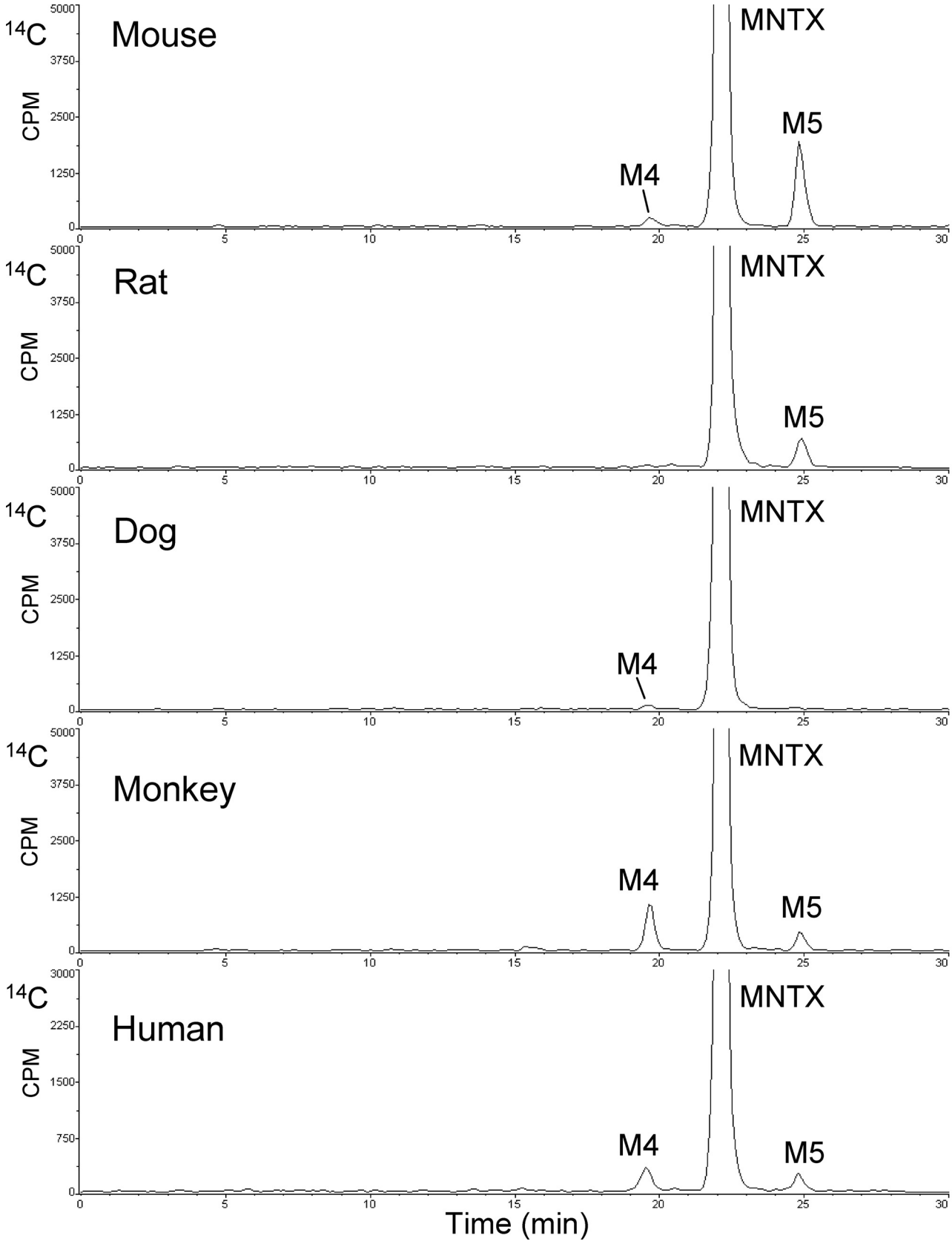

FIG. 1. Radiochromatograms of [^{14}C]MNTX (50 μM) incubated with liver cytosol (4 mg/ml) for 2 h in the presence of NADPH.

4-methylpyrazole was dissolved in 9% dimethyl sulfoxide in water; dicumarol was dissolved in 1% sodium hydroxide in water; and medroxyprogesterone acetate was dissolved in chloroform. Other chemical inhibitors were dissolved in methanol or water. Organic solvent in the incubations was controlled within 2% of the incubation volume. Control incubations were conducted with the vehicles but in absence of the chemical inhibitors. Positive control incubations with human liver cytosol (1.0 mg/ml) were conducted for 1 h with naltrexone (100 μM) as the substrate in place of MNTX. The samples were prepared and analyzed by HPLC with radioactivity flow detection for MNTX and UV detection at 280 nm for naltrexone. Duplicate incubations were prepared for each condition.

HPLC. A Waters (Milford, MA) model 2695 HPLC system with a built-in autosampler was used for analysis. Separations were accomplished on a Luna C18(2) column (250 × 4.6 mm, 5 μm) (Phenomenex, Torrance, CA). The sample chamber in the autosampler was maintained at 4°C, whereas the column was at 40°C. The mobile phase consisted of 0.05% trifluoroacetic acid in water (A) and 0.05% trifluoroacetic acid in methanol (B) and was delivered at 0.6 ml/min. The linear HPLC gradient started at 10% B and increased to 20% over 25 min and then increased to 30% over 5 min. A Flo-One β Model A525 radioactivity flow detector (PerkinElmer Life and Analytical Sciences) with a 250-μl LQTR flow cell and a Waters model 996 photodiode array UV detector set to monitor at 280 nm were used for data acquisition. The flow rate of Ultima Flo M scintillation fluid (PerkinElmer Life and Analytical Sciences) was 3.0 ml/min, providing a mixing ratio of scintillation mixture to mobile phase of approximately 5:1.

Mass Spectrometry. Liquid chromatography/mass spectrometry (LC/MS) analysis used an Agilent Technologies (Santa Clara, CA) model 1100 HPLC system including a binary pump and diode array UV detector. The UV detector was set to monitor λ between 190 and 600 nm. Separations were accomplished under the same conditions as described above, except that a Luna C18(2) column (250 × 2.0 mm, 5 μm; Phenomenex) column was used at ambient temperature of approximately 20°C, and the mobile phase was delivered at 0.3 ml/min.

For hydrogen-deuterium exchange experiments, deuterium oxide was substituted for water in mobile phase A, and d_4-methanol was substituted for methanol in mobile phase B. During LC/MS sample analysis, up to 10 min of the initial flow was diverted away from the mass spectrometer before evaluation of metabolites.

Mass spectral data for the metabolites were obtained with a Micromass quadrupole-time of flight API-US mass spectrometer (Waters). It was equipped with an electrospray ionization source and operated in the positive ionization mode. Full-scan spectra were acquired from *m/z* 100 to 1500 with a scan time of 0.9 s. The capillary and cone voltages were 3.5 kV and 25 V, respectively. The source block and desolvation gas temperatures were 120 and 350°C, respectively. The desolvation gas flow was 900 l/h, and the time of flight-MS resolution was approximately 8000 (m/Δm). Argon was used for collision-activated dissociation experiments at a pressure setting of 13 psig, and the collision offset for acquiring tandem mass spectra varied between 20 and 35 eV, depending on the metabolite.

Isolated metabolite M2 was also analyzed using a TriVersa NanoMate chip-based electrospray ionization system (Advion BioSciences, Inc., Ithaca, NY). A backpressure of approximately 25 psi was used, and the voltage to the electrospray ionization chip was 1.7 kV. Precleaned V-bottomed 96-well storage plates (Advion BioSciences, Inc.) were used to hold the sample before introduction to the mass spectrometer. Metabolite M2 was isolated from SULT2A1 and SULT1E1 incubations and desalted using C18 ZipTips (Millipore Corporation) before being introduced to the mass spectrometer by flow infusion at approximately 50 to 150 nl/min.

TABLE 3

Retention times and mass spectral properties for MNTX and its metabolites observed in liver cytosol and enzyme preparations

Metabolite	t_R	Molecular Ion (M^+)		Relevant Product Ions
		With H_2O	With D_2O	
	min	*m/z*	*m/z*	*m/z*
MNTX	23.0	356	358	338, 302, 284, 227, 199, 112, 55
M2	14.0	436	438	418, 382, 356, 302, 284, 227, 199, 112, 55
M4	20.5	358	361	340, 304, 286, 229, 201, 112, 55
M5	25.5	358	361	340, 304, 286, 229, 201, 112, 55

Results

Carbonyl Reduction of MNTX In Vitro by Hepatic Cytosol of Mice, Rats, Monkeys, and Humans. MNTX reduction metabolites methyl-6α-naltrexol (M4) and methyl-6β-naltrexol (M5) were detected in human hepatic cytosol but not in hepatic or intestinal microsomes or intestinal cytosol when MNTX was incubated in the presence of the NADPH-regenerating system. When MNTX was incubated with human hepatic cytosol in the presence of NADPH, slightly lower activity was observed than with the NADPH-regenerating system, whereas metabolites were not detected when NADH was used as the cofactor (data not shown).

Species differences were observed in metabolite profiles in liver cytosol (Fig. 1) and were generally consistent with previous in vivo metabolism observations (Chandrasekaran et al., 2010). Metabolites formed in liver cytosol were identified by LC/MS and had the same retention times and mass spectra as those observed in human plasma as described elsewhere (Chandrasekaran et al., 2010). Mass spectra data for MNTX and its metabolites identified in liver cytosol and enzyme preparations are summarized in Table 3. In mouse, monkey, and human liver cytosol, both M4 and M5 were observed. However, M4 was observed in greater amounts than M5 in the monkey and human cytosol but in much lower amounts than M5 in mouse liver cytosol. Only M5 was observed in rat liver cytosol, and only a trace amount of M4 was observed in dog liver cytosol. Because of the low activity, a kinetic study was not conducted with dog liver cytosol. The capacity (V_{max}/K_m) for the formation of M4 was much greater in the monkey and human liver cytosol than in the mouse and rat liver cytosol, whereas the capacity for the formation of M5 was greater in mouse liver cytosol than in liver cytosol of other species (Table 4).

TABLE 4

Kinetic parameters for the formation of M4 and M5 from MNTX by liver cytosol of mice, rats, monkeys, and humans, and of 6β-naltrexol from naltrexone by human liver cytosol

Substrate	Species	K_m		V_{max}		V_{max}/K_m	
		M4	M5	M4	M5	M4	M5
		μM	*μM*	*pmol/min/mg*	*pmol/min/mg*	*ml/min/mg*	*ml/min/mg*
MNTX	Mouse	1220	714	11.0	125	0.009	0.175
	Rat	N.D.	396	N.D.	40.7	N.D.	0.103
	Monkey	391	266	80.0	21.9	0.20	0.082
	Human	361	793	43.7	62.5	0.12	0.079
6β-Naltrexol	Human			625		12.6	
Naltrexone	Human	49.7					

N.D., metabolite not detected.

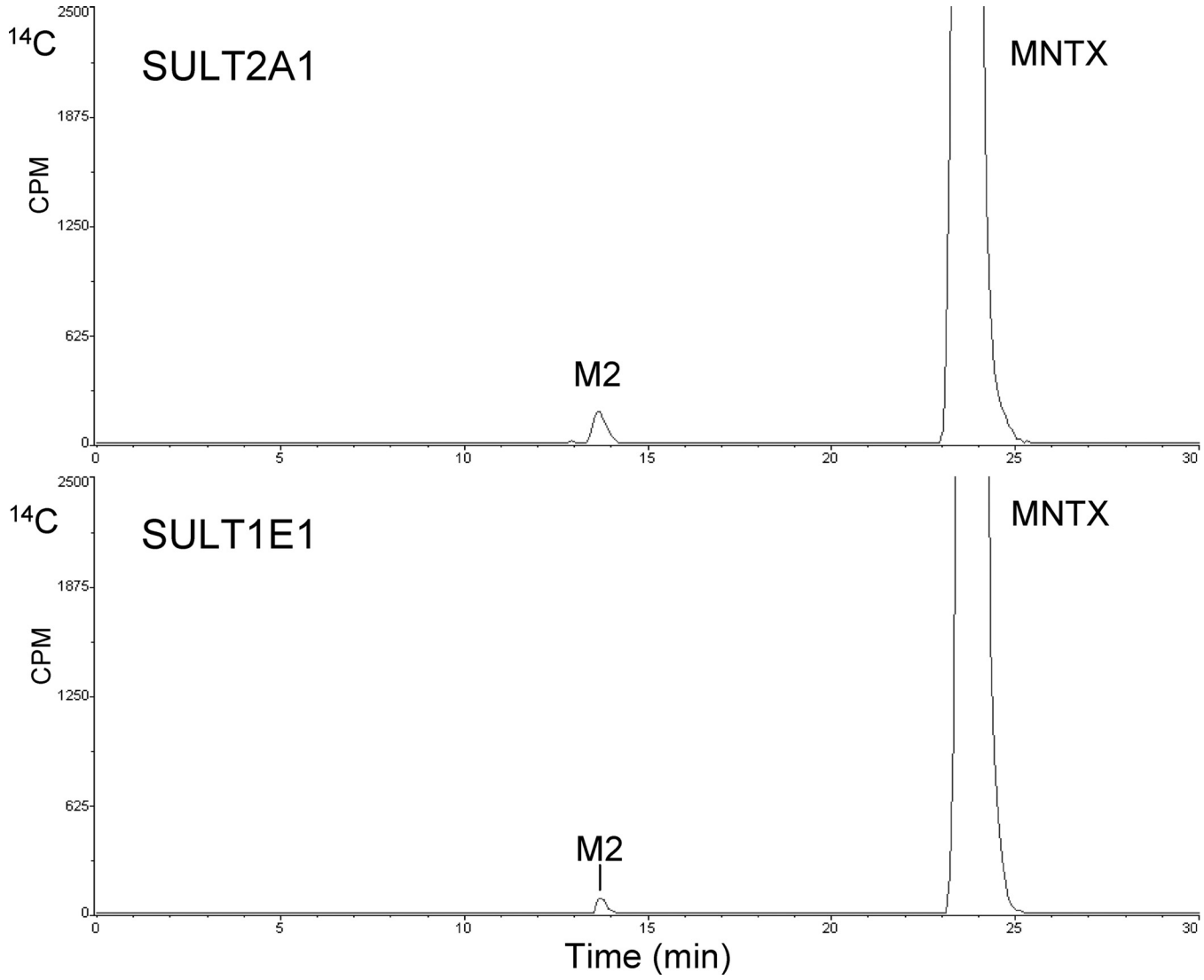

FIG. 2. Formation of M2 by sulfotransferase isoforms SULT2A1 and SULT1E1.

Identification of Sulfotransferase Isoforms for MNTX Sulfation. When [^{14}C]MNTX was incubated with recombinant human sulfotransferases under the conditions used in the present study, MNTX-3-sulfate (M2) was observed as the only product catalyzed by SULT2A1 and SULT1E1 (Fig. 2). The identity of the M2 metabolite peak was confirmed by MS compared with the synthetic standard of M2 (Chandrasekaran et al., 2010). No products were detected when [^{14}C]MNTX was incubated with SULT1A1, SULT1A2, and SULT1A3.

Characterization and Identification of the Enzymes for MNTX Reduction. MNTX reduction to M4 and M5 and naltrexone reduction to 6β-naltrexone in human liver cytosol were most effectively (up to 98%) inhibited by phenolphthalein in a concentration-dependent manner (Table 5). 5β-Cholanic acid-3α,7α-diol and medroxyprogesterone moderately inhibited the MNTX reduction by up to 67%. 5β-Cholanic acid-3α,7α-diol and medroxyprogesterone also inhibited naltrexone reduction. Moderate inhibition of the reduction of MNTX and naltrexone was observed with ethacrynic acid, menadione, and quercetin. No inhibition of the reduction of MNTX or naltrexone was observed with 4-methlpyrazole and phenobarbital at concentrations up to 100 μM. Whereas formation of M5 was moderately inhibited by flufenamic acid, slightly inhibited by indomethacin, and unchanged by dicumarol, formation of M4 was increased 2.1-, 1.4-, and 1.9-fold in a concentration-dependent manner by flufenamic acid, indomethacin, and dicumarol, respectively (data not shown). These three chemical inhibitors showed no inhibitory effect on the reduction of naltrexone.

TABLE 5

Percentage of inhibition of the formation of M4 and M5 from MNTX, and of 6β-naltrexol from naltrexone by chemical inhibitors

Inhibitor concentration (μM)	M4		M5		6β-Naltrexol	
	10	100	10	100	10	100
Phenolphthalein	81	89	76	97	75	98
Flufenamic acid	N.I.	N.I.	25	53	2	11
5β-Cholanic acid-3α,7α-diol	21	39	46	67	10	34
Medroxyprogesterone acetate	28	59	36	67	31	47
Indomethacin	1	N.I.	9	34	N.I.	6
Phenobarbital	N.I.	2	N.I.	N.I.	2	N.I.
Ethacrynic acid	8	27	13	48	4	31
Menadione	6	35	N.I.	43	7	26
Quercetin	4	28	7	46	9	32
4-Methylpyrazole	4	6	5	15	N.I.	9
Dicumarol	N.I.	N.I.	4	N.I.	1	11

N.I., no inhibition.

Discussion

The primary metabolic pathways for MNTX in humans are sulfation and carbonyl reduction (Chandrasekaran et al., 2010). MNTX was metabolized via glucuronidation, hydroxylation, methylation, sulfation, and carbonyl reduction in nonhuman species. The species differences in the carbonyl reduction of MNTX by hepatic cytosol in the presence of NADPH were consistent with the in vivo data in mice, rat, dogs, and humans. Both M4 and M5 were formed in liver cytosol of mice and humans. However, M4 was observed in a higher amount than M5 in human liver cytosol, which was consistent with human plasma profiles, whereas M4 was a minor isomer in mouse liver cytosol. Only trace amounts of M4 were observed in dog liver cytosol. The kinetic parameters in human liver cytosol also showed that the capacity for carbonyl reduction was approximately 100-fold greater for naltrexone than for MNTX. The kinetic data for the formation of 6β-naltrexol from naltrexone in human liver cytosol were also consistent with a literature report by Porter et al. (2000).

Of the five recombinant human sulfotransferase enzymes examined, only SULT1E1 and SULT2A1 catalyzed MNTX sulfation. SULT1E1 expressed in human liver and jejunum is important for steroid homeostasis (Gamage et al., 2006) and also has high affinity for β-estradiol, estrone, and a number of synthetic estrogens (Gamage et al., 2006). SULT2A1, which is present in human liver, adrenal, small intestine, and other organs, is responsible for the sulfation of hydroxysteroids, including dehydroepiandrosterone, androgens, pregnenolone, and bile acids (Gamage et al., 2006). SULT1A1, SULT1A2, and SULT1A3, which are responsible for sulfation of phenolic compounds and catecholamines, showed no activity toward MNTX.

Carbonyl reduction of MNTX was catalyzed by NADPH-dependent cytosolic enzymes in human liver. The enzymes responsible for MNTX reduction were identified by using selective chemical inhibitors of AKR isoforms, CR/SDR, alcohol dehydrogenase, and quinone oxidoreductase. The reduction of both MNTX and naltrexone was most effectively inhibited by phenolphthalein, which inhibits AKR1C isoforms with better selectivity toward AKR1C4 than for AKR1C1, AKR1C2, or AKR1C3 (Steckelbroeck et al., 2006). Naltrexone reduction has been shown to be catalyzed by AKR1C4, with minor contribution from AKR1C1 and AKR1C2 (Breyer-Pfaff and Nill, 2004). Formation of M4 and M5 was inhibited by up to 67% by the AKR1C2-selective inhibitor 5β-cholanic acid-3α,7α-diol (Breyer-Pfaff and Nill, 2004) and by medroxyprogesterone acetate, which inhibits AKR1C1, AKR1C2, and AKR1C4 (Atalla et al., 2000). 5β-Cholanic acid-3α,7α-diol and medroxyprogesterone acetate inhibited naltrexone reduction by approximately 34 and 47% at 100 μM, respectively. Flufenamic acid, a selective inhibitor of AKR1C1, AKR1C2, and AKR1C3 and a weak inhibitor of AKR1C4 (Steckelbroeck et al., 2004, 2006), inhibited the formation of M5 but increased the formation of M4 up to 2.1-fold in a concentration-dependent manner, whereas little inhibitory effect was observed on 6β-naltrexol formation. Indomethacin is an unspecific inhibitor of both AKRs and CR and showed low to moderate potency with either substrate (Gebel and Maser, 1992; Maser et al., 2000). Indomethacin had no inhibitory effect on 6β-naltrexol formation, slightly inhibited M5 formation, but increased M4 formation. The lack of inhibitory effect by phenobarbital (an inhibitor of AKR1A1 and AKR1B1) on the reduction of MNTX and naltrexone confirmed that the AKRs capable of reducing xenobiotic ketones are primarily the AKR1C subfamily in humans (Atalla et al., 2000). Altogether, the data indicated that multiple isoforms in the AKR1C subfamily are responsible for MNTX reduction, with major contribution probably from AKR1C4, which is virtually liver-specific (Penning et al., 2000).

Ethacrynic acid, menadione, and quercetin, the inhibitors of CR or SDR (Maser et al., 2000; Rosemond et al., 2004), did not appear to affect the reduction of either MNTX or naltrexone significantly. Because Breyer-Pfaff and Nill (2004) have shown that CR was not involved in the reduction of naltrexone, the decreases in the reduction of MNTX and naltrexone may be a result of nonspecific inhibition by these inhibitors. Incubations with the chemical inhibitors (4-methylpyrazole and dicumarol, respectively) of alcohol dehydrogenase and quinone oxidoreductase showed that these two enzymes are not involved in the reduction of MNTX. However, the quinone oxidoreductase inhibitor dicumarol increased M4 formation by 1.9-fold at 100 μM, similar to flufenamic acid.

Stereoselective effects on MNTX reduction were observed with flufenamic acid, indomethacin, and dicumarol. Whereas they inhibited the formation of the 6β-epimer, they enhanced the formation of the 6α-epimer. Such effects of these inhibitors were not observed with naltrexone because it was reduced only to one epimer, 6β-epimer. Enzyme activation in vitro has been well documented for cytochrome P450 (P450) isoforms, particularly CYP3A (Fayz and Inaba, 1998). Various mechanisms have been proposed for the activation of P450

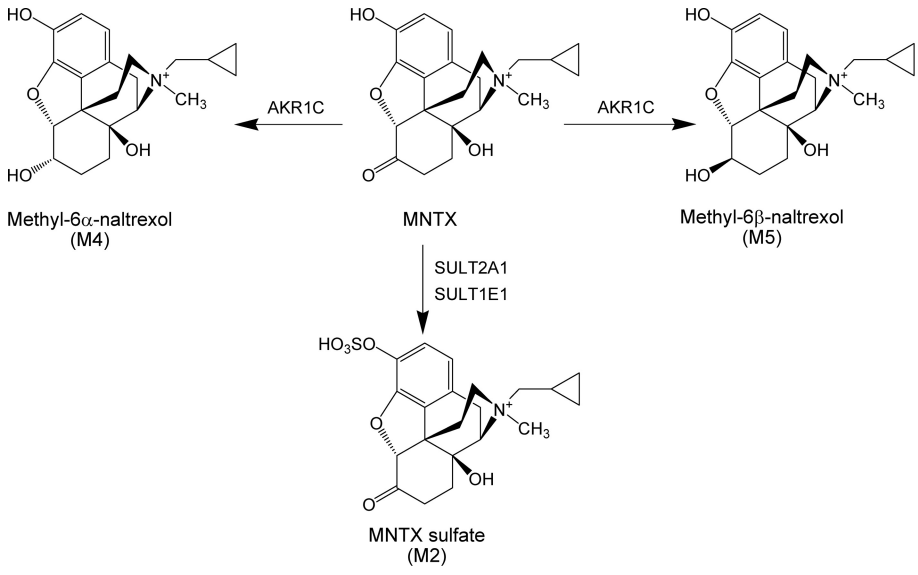

FIG. 3. Metabolic pathways of MNTX in humans.

enzymes. An activator such as 7,8-benzoflavone may enhance the interaction of P450 reductase and P450 (Huang et al., 1981). Flavones are allosteric effectors that may increase catalytic efficiency by decreasing the K_m and increasing the V_{max} (Schwab et al., 1988). Shou et al. (1994) showed simultaneous binding of two substrates to the P450 active site. Binding of a substrate to the active site can alter the orientation of another substrate, thereby changing the regioselectivity of the metabolism. Enzyme activation of P450 reductase and cytochrome b_5 reductase by ethacrynic acid, dipyridamole, and indomethacin has also been reported for the reduction of 3′-azido-3′-deoxythymidine to 3′-amino-3′-deoxythymidine (Fayz and Inaba, 1998). However, activation of AKR enzyme activity has not been reported. AKRs share a common $(\alpha/\beta)_8$-barrel three-dimensional fold, with highly conserved nicotinamide-cofactor-binding pocket and active site (Jez et al., 1997; Sanli et al., 2003). Jez et al. (1997) proposed that the three loops on the C-terminal side of the barrel play potential roles in determining the positional and stereospecificity of the reaction. Studies have shown that the active site of AKRs adapts itself to bind tightly to different inhibitors (Urzhumtsev et al., 1997; El-Kabbani et al., 1998). Lovering et al. (2004) examined the X-ray crystal structures of AKR1C3 complexed with indomethacin or flufenamic acid. One molecule of indomethacin is bound in the active site, whereas flufenamic acid binds to both the active site and the β-hairpin loop at the opposite end of the central β-barrel. It is not clear how flufenamic acid, indomethacin, and dicumarol interact with the enzymes and change the stereochemistry to have differential effects on the formation of the 6α- and 6β-epimers. Because these effects were not observed with naltrexone, the methyl group and charge in the molecule of MNTX may have contributed to the observations.

In summary, sulfation and carbonyl reduction are the major metabolic pathways for MNTX in humans (Fig. 3). Species differences observed in the carbonyl reduction of MNTX to M4 and M5 in hepatic cytosol were consistent with previously reported in vivo metabolite profiles. The present study identified SULT2A1 and SULT1E1 as the sulfotransferases involved in the sulfation of MNTX in humans. AKR1C4 appeared to play a major role in the carbonyl reduction of MNTX, although multiple enzymes in the AKR1C subfamily may be involved in the reduction. Carbonyl reductase may have no or limited contribution to MNTX reduction. The mechanism of the activation of the formation of M4 while inhibiting the formation of M5 by flufenamic acid, indomethacin, and dicumarol warrants further investigation.

Acknowledgments. We thank Daniel Evcic for technical contributions to this study.

References

Atalla A, Breyer-Pfaff U, and Maser E (2000) Purification and characterization of oxidoreductases-catalyzing carbonyl reduction of the tobacco-specific nitrosamine 4-methylnitrosamino-1-(3-pyridyl)-1-butanone (NNK) in human liver cytosol. *Xenobiotica* **30:**755–769.

Atalla A and Maser E (2001) Characterization of enzymes participating in carbonyl reduction of 4-methylnitrosamino-1-(3-pyridyl)-1-butanone (NNK) in human placenta. *Chem Biol Interact* **130–132:**737–748.

Bauman DR, Rudnick SI, Szewczuk LM, Jin Y, Gopishetty S, and Penning TM (2005) Development of nonsteroidal anti-inflammatory drug analogs and steroid carboxylates selective for human aldo-keto reductase isoforms: potential antineoplastic agents that work independently of cyclooxygenase isozymes. *Mol Pharmacol* **67:**60–68.

Breyer-Pfaff U and Nill K (2004) Carbonyl reduction of naltrexone and dolasetron by oxidoreductases isolated from human liver cytosol. *J Pharm Pharmacol* **56:**1601–1606.

Brown DR and Goldberg LI (1985) The use of quaternary narcotic antagonists in opiate research. *Neuropharmacology* **24:**181–191.

Chandrasekaran A, Tong Z, Li H, Erve J, DeMaio W, Goljer I, McConnell O, Rotshteyn Y, Hultin T, Talaat R, et al. (2010) Metabolism of intravenous methylnaltrexone in mice, rats, dogs and humans. *Drug Metab Dispos* doi: 10.1124/dmd.109.031179.

El-Kabbani O, Wilson DK, Petrash M, and Quiocho FA (1998) Structural features of the aldose reductase and aldehyde reductase inhibitor-binding sites. *Mol Vis* **4:**19.

Fayz S and Inaba T (1998) Zidovudine azido-reductase in human liver microsomes: activation by ethacrynic acid, dipyridamole, and indomethacin and inhibition by human immunodeficiency virus protease inhibitors. *Antimicrob Agents Chemother* **42:**1654–1658.

Gamage N, Barnett A, Hempel N, Duggleby RG, Windmill KF, Martin JL, and McManus ME (2006) Human sulfotransferases and their role in chemical metabolism. *Toxicol Sci* **90:**5–22.

Gebel T and Maser E (1992) Characterization of carbonyl reducing activity in continuous cell lines of human and rodent origin. *Biochem Pharmacol* **44:**2005–2012.

Huang MT, Chang RL, Fortner JG, and Conney AH (1981) Studies on the mechanism of activation of microsomal benzo[a]pyrene hydroxylation by flavonoids. *J Biol Chem* **256:**6829–6836.

Jez JM, Bennett MJ, Schlegel BP, Lewis M, and Penning TM (1997) Comparative anatomy of the aldo-keto reductase superfamily. *Biochem J* **326:**625–636.

Lovering AL, Ride JP, Bunce CM, Desmond JC, Cummings SM, and White SA (2004) Crystal structures of prostaglandin D(2) 11-ketoreductase (AKR1C3) in complex with the nonsteroidal anti-inflammatory drugs flufenamic acid and indomethacin. *Cancer Res* **64:**1802–1810.

Maser E, Stinner B, and Atalla A (2000) Carbonyl reduction of 4-(methylnitrosamino)-1-(3-pyridyl)-1-butanone (NNK) by cytosolic enzymes in human liver and lung. *Cancer Lett* **148:**135–144.

Matsunaga T, Shintani S, and Hara A (2006) Multiplicity of mammalian reductases for xenobiotic carbonyl compounds. *Drug Metab Pharmacokinet* **21:**1–18.

Penning TM, Burczynski ME, Jez JM, Hung CF, Lin HK, Ma H, Moore M, Palackal N, and Ratnam K (2000) Human 3alpha-hydroxysteroid dehydrogenase isoforms (AKR1C1-AKR1C4) of the aldo-keto reductase superfamily: functional plasticity and tissue distribution reveals roles in the inactivation and formation of male and female sex hormones. *Biochem J* **351:**67–77.

Porter SJ, Somogyi AA, and White JM (2000) Kinetics and inhibition of the formation of 6beta-naltrexol from naltrexone in human liver cytosol. *Br J Clin Pharmacol* **50:**465–471.

Rosemond MJ, St John-Williams L, Yamaguchi T, Fujishita T, and Walsh JS (2004) Enzymology of a carbonyl reduction clearance pathway for the HIV integrase inhibitor, S-1360: role of human liver cytosolic aldo-keto reductases. *Chem Biol Interact* **147:**129–139.

Rosemond MJ and Walsh JS (2004) Human carbonyl reduction pathways and a strategy for their study in vitro. *Drug Metab Rev* **36:**335–361.

Sanli G, Dudley JI, and Blaber M (2003) Structural biology of the aldo-keto reductase family of enzymes: catalysis and cofactor binding. *Cell Biochem Biophys* **38:**79–101.

Schwab GE, Raucy JL, and Johnson EF (1988) Modulation of rabbit and human hepatic cytochrome P-450-catalyzed steroid hydroxylations by alpha-naphthoflavone. *Mol Pharmacol* **33:**493–499.

Shou M, Grogan J, Mancewicz JA, Krausz KW, Gonzalez FJ, Gelboin HV, and Korzekwa KR (1994) Activation of CYP3A4: evidence for the simultaneous binding of two substrates in a cytochrome P450 active site. *Biochemistry* **33:**6450–6455.

Steckelbroeck S, Jin Y, Gopishetty S, Oyesanmi B, and Penning TM (2004) Human cytosolic 3alpha-hydroxysteroid dehydrogenases of the aldo-keto reductase superfamily display significant 3beta-hydroxysteroid dehydrogenase activity: implications for steroid hormone metabolism and action. *J Biol Chem* **279:**10784–10795.

Steckelbroeck S, Oyesanmi B, Jin Y, Lee SH, Kloosterboer HJ, and Penning TM (2006) Tibolone metabolism in human liver is catalyzed by 3alpha/3beta-hydroxysteroid dehydrogenase activities of the four isoforms of the aldo-keto reductase (AKR)1C subfamily. *J Pharmacol Exp Ther* **316:**1300–1309.

Urzhumtsev A, Tête-Favier F, Mitschler A, Barbanton J, Barth P, Urzhumtseva L, Biellmann JF, Podjarny A, and Moras D (1997) A 'specificity' pocket inferred from the crystal structures of the complexes of aldose reductase with the pharmaceutically important inhibitors tolrestat and sorbinil. *Structure* **5:**601–612.

Wall ME, Brine DR, and Perez-Reyes M (1981) Metabolism and disposition of naltrexone in man after oral and intravenous administration. *Drug Metab Dispos* **9:**369–375.

Wall ME, Perez-Reyes M, Brine DR, and Cook CE (1984) Naltrexone disposition in man after subcutaneous administration. *Drug Metab Dispos* **12:**677–682.

Yuan CS, Foss JF, O'Connor M, Moss J, and Roizen MF (1998) Gut motility and transit changes in patients receiving long-term methadone maintenance. *J Clin Pharmacol* **38:**931–935.

Yuan CS, Foss JF, O'Connor M, Osinski J, Karrison T, Moss J, and Roizen MF (2000) Methylnaltrexone for reversal of constipation due to chronic methadone use: a randomized controlled trial. *JAMA* **283:**367–372.

Yuan CS, Foss JF, O'Connor M, Osinski J, Roizen MF, and Moss J (1999) Effects of intravenous methylnaltrexone on opioid-induced gut motility and transit time changes in subjects receiving chronic methadone therapy: a pilot study. *Pain* **83:**631–635.

Yuan CS, Foss JF, O'Connor M, Toledano A, Roizen MF, and Moss J (1996) Methylnaltrexone prevents morphine-induced delay in oral-cecal transit time without affecting analgesia: a double-blind randomized placebo-controlled trial. *Clin Pharmacol Ther* **59:**469–475.

Yuan CS, Wei G, Foss JF, O'Connor M, Karrison T, and Osinski J (2002) Effects of subcutaneous methylnaltrexone on morphine-induced peripherally mediated side effects: a double-blind randomized placebo-controlled trial. *J Pharmacol Exp Ther* **300:**118–123.

Address correspondence to: Appavu Chandrasekaran, Pfizer Inc., 500 Arcola Road, Collegeville, PA 19426. E-mail: chandra@wyeth.com